

# Investigation of the three dimensional flow structures in a planar offset attaching jet

Nan Gao

*State Key Lab of Structural Analysis, School of Aeronautics, Dalian University of Technology, Dalian, China*

Dan Ewing

*Toronto, Canada*

**An experimental investigation was performed to characterize the three dimensionality of the flow structures in a planar offset jet initially issuing parallel to an adjacent wall with an offset distance of 1 jet height and a Reynolds number of 44 000. The results showed that the flow structures in the shear layers of the attaching jet were initially three dimensional with spanwise length scale of 1 to  $2H_j$  in the attachment region. The flow structures in the outer shear layer grew as they evolved downstream and induced two dimensional near wall motions in the transitional region and developed wall jet region.**

## I. Introduction

Offset attaching planar jets, formed when a planar jet develops near a wall, occur in a number of practical applications and have been the subject of a number of investigations.<sup>1-6</sup> The measurements show that offset jets initially attach to the wall and then transition to a wall jet. The development of the flow in each region at least in the case of small initial offset distances can be characterized in terms of local characteristics length and velocity scales.<sup>5</sup> For the small initial offset distances of interest here ( $H_s \lesssim H_j$ ), the inner shear layer of the jet interacts with the wall before the outer shear layer and thus, the structures near the wall are initially higher frequency motions from this shear layer.<sup>5</sup> The structures transition to lower frequency wall jet motions that appear to form in the outer shear of the attaching jet as the flow transitions to the wall jet in the region  $6 \lesssim x/H_j \lesssim 10$ . The two-time correlation between the fluctuating wall pressure and the fluctuating velocity field show evidence that both structures were present in this transition region with the higher frequency motions near the wall and the lower frequency motions further away from the wall. The lower frequency wall jet motions approach the wall and eventually dominate the flow as the flow transitions to a wall jet flow.<sup>5</sup>

Gao and Ewing<sup>6</sup> considered the cross spectra between the fluctuating wall pressure and the fluctuating velocities in the offset jets with  $H_s/H_j = 1.0$  and found evidence of more motions playing a role in this flow. In particular, they found evidence of a lower frequency flapping motion in the attaching region typical of attaching shear layer flows, low frequency motions associated with the recirculating region below the jet, and evidence of two different higher frequency motions in the attached shear layer. Gao and Ewing<sup>6</sup> proposed that the two different frequency shear layer motions may be associated with the different trajectory of the shear layer toward the wall due to the flapping of the shear layer. The measurements also showed the transition to the wall jet motions and a change in the phase velocity of these motions relative to the upstream motions. The analysis of the different motions was based on two-dimensional measurements (separation distances in the streamwise and normal directions) and the three-dimensional character of the different motions has not been considered.

The three-dimensional nature of the motions in attaching shear layer flows have been considered previously.<sup>7,8</sup> For example, Lee and Sung<sup>7</sup> considered the spanwise correlation of the surface wall pressure fluctuations and the velocity fluctuations at different spanwise locations in the flow over a backward facing step and found that the spanwise length scale of the flow structures in the separated shear layer grew as they approached the reattachment region. Numerical investigations of the three dimensionality of a turbulent wall<sup>9,10</sup> showed evidence of a highly two-dimensional motions and thus, it is expected that there will be a

change in the three-dimensional character of the motions in the offset attaching jet as it transitions from the attaching region to the wall jet region.

The objective of this investigation was to characterize the three dimensionality of the large scale flow structures in an offset jet downstream of the attachment point to examine the change in the three-dimensionality of the structures as the flow transitions from an attaching jet to the wall jet. The three-dimensionality of the structures in a jet with  $H_s/H_j = 1$  was examined by characterizing the correlation between the fluctuating wall pressure and the fluctuating velocity using approach similar to Lee and Sung.<sup>7</sup> The cross-spectra are also examined to characterize the contributions of the different frequency ranges following Gao and Ewing.<sup>6</sup> Measurements were taken at a point immediately downstream of the reattachment point, at a points in the transition region between the attaching jet and wall jet flows, and at a point where the wall jet structures are dominant. The experimental facilities and methodology used in this investigation are outlined in the next section. The two-point correlations are then presented and discussed followed by the cross-spectra.

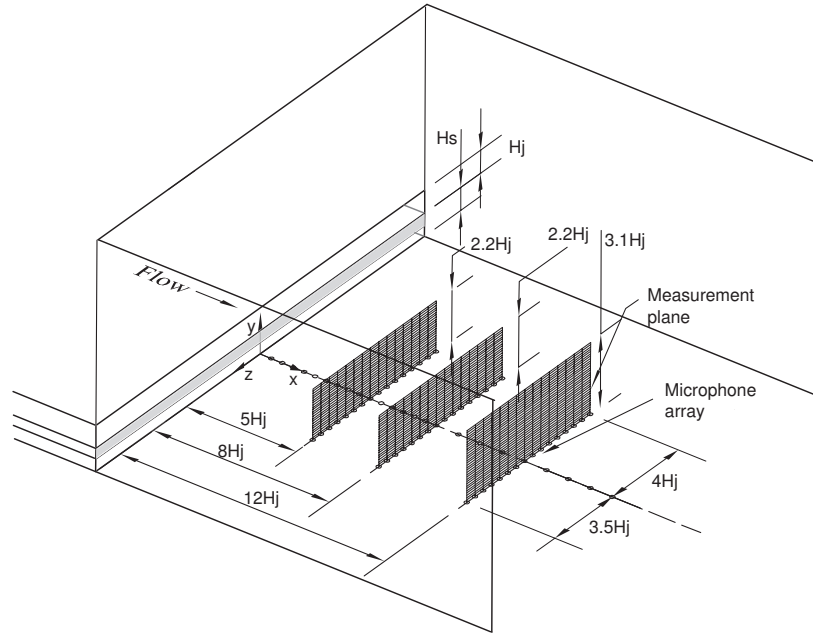


Figure 1. Schematics of the experimental setup.

## II. Experimental Methodology

The measurements were performed using a facility shown in figure 1 (also used in Gao & Ewing<sup>5</sup>) that consisted of an upper and a lower channel. Flow exited only the upper channel, the exit of the lower channel was blocked in this study. The air flow supplied from a variable speed blower passed through a large upper settling chamber (122 cm by 72.4 cm by 45.7 cm) that included layers of foam and perforated plates to condition the flow. The inlet on the settling chambers included gate valves to adjust the flow rate. The flow exiting the settling chamber entered the upper channel with a width of 74.3 cm. The height of the upper channel,  $H_j$ , was 3.8 cm, while the length of the upper channel was 81 cm. The distance from the lower edge of the upper channel to the wall was 3.8 cm. The Reynolds number of the jet (based on the jet height and the averaged velocity at the jet exit) was 44000. The profiles of mean velocity and turbulent stresses measured near the exit of the channel were symmetric and similar to a fully developed channel flow.<sup>6</sup> The flow exiting the channel developed over a 1.8m long plate that was mounted parallel to the channel. The flow was confined by a wall over the channel and two side walls to a height of approximately 90 cm above the bottom wall.

The flow field was measured using single and cross hot-wire probes with an in-house anemometry system. The sensor in the probes had a diameter of  $5\mu\text{m}$  and lengths of 1.25mm and 1.5mm, respectively. The hot wire probes were calibrated in a jet exiting a round contoured nozzle with a uniform exit velocity profile. The resulting response curves were fit with a fourth-order polynomial, and a modified cosine law.<sup>13</sup> The flow

field was measured by moving the hot-wire probe on a computer controlled traverse that could be positioned with an accuracy less than 0.05mm.

The pressure fluctuations on the bottom wall was measured using 16 Panasonic WM-60B microphones, that had flat responses for 20Hz to 5000Hz. The microphones were mounted directly into blind cavities drilled from the bottom of the wall. The microphones sensed the flow through a 1mm-diameter, 5mm-long pinhole drilled through the wall to the top of the cavity. The facility included a series of holes on a line 0.75 cm from the facility centerline used in Gao and Ewing.<sup>5,6</sup> A series of measurement locations were added across the jet at three streamwise locations  $x/H_j = 5, 8$  and  $12$  for this investigation. The locations had a lateral spacing of 1.9 cm (or  $0.5 H_j$ ) and covered  $-3.5 \leq z/H_j \leq 4$  where  $z/H_j = 0$  was the location of the streamwise microphone array. The microphones for these measurements were calibrated externally with a piston phone at 1000Hz.

Two separate sets of experiments were performed to characterize the two-point correlations in the flow following a similar approach to Lee and Sung.<sup>7</sup> In one set of experiment, the 16-microphone array was used to simultaneously measure the fluctuating wall pressure at different lateral positions across the flow at  $x/H_j = 5, 8$  and  $12$ . In the second set of experiments, a cross wire probe was used to measure the streamwise and vertical velocity components at 21 vertical locations over each of the microphones as shown in figure 1 simultaneous with the pressure measurements. Experiments were performed for two different cross-wire orientations to capture all three components. Gao and Ewing<sup>5,6</sup> previously performed similar experiments using the pressure measurement locations in the streamwise direction and that data was considered here.

The output signals from the anemometers and the microphones were sampled simultaneously in each of the experiment using a 14-bit A/D board at a frequency of 2048Hz for a total time of 75 seconds. The uncertainties in the mean velocity and rms velocity measurements due to sample size evaluated following the approach in Bruun<sup>13</sup> were less than 1% and 3% for a 95% confidence interval. The uncertainty in the cross-spectra were 8%, while the uncertainties in the coherence and phase computed from these cross-spectra were 53% and 38% when the coherence was 0.15, and 12% and 9% when the coherence was 0.5. The uncertainties were estimated following approach given in Bendat and Piersol.<sup>14</sup> The experimental methodologies here follow that for the two dimensional measurements in single offset jets<sup>5,6</sup> and further details can be found there.

### III. Results and Discussions

The profiles of the mean and fluctuating velocities measured in the central part of the jet ( $-4 \leq z/H_j \leq 4$ ) at  $x/H_j = 5, 8$  and  $12$  are shown in figure 2. The profiles at different spanwise locations agreed well indicating that the mean flow of the jet was two dimensional and the side walls had little effect in the region  $-4 \leq z/H_j \leq 4$ . The three dimensionalities of the flow structures in the offset jet were studied using the correlations and the coherence of the fluctuating pressure and velocities, the results were discussed in part I and II, respectively.

#### A. Part I: Correlations

The correlation coefficient of the fluctuating wall pressure

$$\rho_{pp}(x, z_1, z_2, \tau) = \frac{\overline{p(x, z_1, t)p(x, z_2, t + \tau)}}{p'(x, z_1)p'(x, z_2)} \quad (1)$$

were computed from the simultaneous measurements of fluctuating wall pressure using an array of microphones located in the spanwise direction. The flow was homogeneous in the area studied ( $-4 \leq z/H_j \leq 4$ ), thus the results can be presented in terms of  $\Delta z = z_2 - z_1$ . The correlations in the spanwise direction measured at  $x/H_j = 5, 8$  and  $12$  are shown in figure 3. These three locations are in attaching region (region II,  $0.65 < x/X_r \leq 1.1$ ), transition region (region IV,  $6 \leq x/H_j \leq 10$ ) and wall jet region (region V,  $x/H_j > 10$ ), respectively. The correlations show that there are periodic structures in the flow at all these three streamwise locations, the time scales of these structures agreed with the results in Gao and Ewing.<sup>5</sup> The spanwise length scales of the flow structures grew significantly from  $x/H_j = 5$  to  $8$  while the jet developed from the region immediately downstream of the attachment to the transition region. The growth rate of scales was slower from  $x/H_j = 8$  to  $12$ . The changes of the scales of the flow structures suggested the wall jet structures were more two dimensional than the inner shear layer structures.

The correlation coefficients of the fluctuating wall pressure and the fluctuating velocities

$$\rho_{p\alpha}(x, y, \Delta z, \tau) = \frac{\overline{p(x, \Delta z = 0, t)\alpha(x, y, \Delta z, t + \tau)}}{\overline{p'(x, \Delta z = 0)\alpha'(x, y, \Delta z)}} \quad (2)$$

were computed from the simultaneous measurements of the wall pressure using a microphone array and the velocities measured using a cross hot-wire probe traversed in the y-z plane over the microphones. Here,  $\alpha$  is velocity components  $u$ ,  $v$  or  $w$ . The correlations  $\rho_{p\alpha}(x, y, \Delta z)$  at  $x/H_j = 5, 8$  and  $12$  for different intervals are shown in figure 4 to 6. Here, the correlations were symmetrized with respect to the center line  $\Delta z=0$ . The correlations  $\rho_{pu}$  and  $\rho_{pv}$  in the streamwise direction for  $\Delta z = 0$  were computed from the measurements of Gao and Ewing<sup>5</sup> and included. The correlation  $\rho_{pw}$  is zero in this plane because it is anti-symmetric about  $\Delta z = 0$ . The correlation contours on the y-z plane that show the three dimensionality were plot using thicker lines. There are regions with large positive and negative correlations in x-y plane at  $x/H_j = 5$  associated with the passing shear layer structures in the flow. These regions were close to the wall ( $y/H_j \leq 1$ ) suggesting these were the structures in the inner shear layer. The correlations were small in the region  $y/H_j > 1$  suggesting the outer shear layer structures have less impact on the wall pressure at  $x/H_j = 5$ . The correlations of pressure and fluctuating velocities in y-z plane was large in a region above the microphone. The size of the region with good correlation changed with time interval, the changes were more obvious in the contours of  $\rho_{pu}$  suggesting the structures in the inner shear layer were three dimensional.

There was also evidence of inner and outer shear layer structures in the correlations in y-z plane shown at  $x/H_j = 8$  in figure 5. The inner shear layer structures developed near the wall ( $y/H_j < 0.5$ ) and the outer structures away from the wall ( $1 < y/H_j < 2$ ). The spanwise length scale of the outer structures was larger than the inner structures. It should be noted that the results suggested there was a third motion between the inner and outer shear layer structures. This motion has a larger spanwise length scales than both types of shear layer structures. This motion was likely associated with the outer shear layer structures.

Evidence of the inner shear layer structure was not present at  $x/H_j = 12$  shown in figure 6. The motions above and below the wall jet structures also became more obvious than they were in at  $x/H_j = 8$ , particularly the motion between the jet where the spanwise length scale was large. The near wall motion has the largest effect on the wall fluctuating pressure because of the close distance to the wall. The correlations of wall pressure and velocities agree with the results of two-time two-point pressure correlations.

## B. Part II: Coherence and Phase

The spectra of the fluctuating velocities at  $x/H_j = 5, 8$ , and  $12$  are shown in figure 7. The results show that the spectra  $F_{uu}$  at  $x/H_j = 5$  roll near  $fX_r/U_j = 1$  ( $fH_j/U_j \approx 0.21$ ). The characteristic frequency of the outer shear layer decreased gradually to  $fH_j/U_j \approx 0.06$  from  $x/H_j = 5$  to  $12$  as the wall jet structures grew in size.<sup>5</sup> The changes were more obvious in the spectra  $F_{vv}$  and  $F_{ww}$ . Gao and Ewing<sup>6</sup> showed that the analysis of the cross-spectra yielded a more complex picture.

The coherence of the spectra between the fluctuating wall pressure measured at two lateral locations given by

$$\gamma_{pp}(x, \Delta z, f) = \frac{|F_{pp}(x, \Delta z, f)|}{F_{pp}(x, \Delta z = 0, f)}. \quad (3)$$

is shown in Figure. 8. Here,  $F_{pp}(x, \Delta z, f)$  is the cross spectrum of the fluctuating wall pressure between two locations  $\Delta z$  apart and  $F_{pp}(x, \Delta z = 0, f)$  is the pressure spectrum at the location  $(x)$ . The cross-spectra  $F_{pp}(x, \Delta z, f)$  is the average of the results from all locations separated by  $\Delta z$  and the results for positive and negative separations have been symmetrized. The coherence between the wall pressure for separation distances in the streamwise direction reported by Gao and Ewing<sup>6</sup> is included on this figure as a reference. The results at  $x/H_j = 5$  immediately downstream of the reattachment location do not show evidence of strong two-dimensionality consistent with the correlation measurements. The results however do show evidence of a change in the lateral span of good coherence with frequency. The lateral coherence is largest for the motions centered around  $fH_j/U_j \approx 0.07$  that correspond to the wall jet motions and the motions with  $fX_r/U_j \geq 0.6$  that correspond to the shear layer motions. The results for  $x/H_j = 8$  show that there is a significant change in the three-dimensionality associated with the transition to the wall jet structures. The fluctuations at frequencies associated with the wall jet motions ( $0.05 \leq fH_j/H_j \leq 0.08$ ) are coherent over the full range of lateral positions considered here. The coherence does decrease indicating there is a three-dimensional component of this motion. The motions with  $fX_r/U_j > 0.6$  extend over a

smaller lateral region than at  $x/H_j = 5$ . The results at  $x/H_j = 12$  show that the lateral coherence of the pressure fluctuations associated with the wall jet increase at the flow evolves downstream. The phase of the cross-spectra showed that the pressure was in phase over the region of strong coherence.

The three-dimensionality of the different motions was examined by determining the coherence of the pressure and the fluctuating velocity components at different frequency given by

$$\gamma_{p\alpha}(x, y, \Delta z, f) = \frac{|F_{p\alpha}(x, y, \Delta z, f)|}{F_{pp}(x, \Delta z = 0, f)^{1/2} F_{\alpha\alpha}(x, y, \Delta z, f)^{1/2}}. \quad (4)$$

where  $\alpha$  is the  $u$ ,  $v$ , or  $w$  velocity component. Gao and Ewing<sup>6</sup> found that there was evidence of two different types of shear layer motions; motions with frequencies of  $1 \leq fX_r/U_j \leq 1.4$  that appear related to the structures in the upstream shear layer and motions with lower frequencies of  $0.6 \leq fX_r/U_j \leq 0.9$  that appear to form in the region where the shear layer interacts with the wall. The lateral coherence of the pressure and velocity fluctuations for these ranges were both examined here. The streamwise locations of the reference microphone were different from those considered in Gao and Ewing<sup>6</sup> so the coherence between the wall pressure and velocity for separation distance in the streamwise direction for  $\Delta z = 0$  were computed from the measurements in Gao and Ewing<sup>6</sup> and included in the figure. The results for frequencies in these ranges and in the typical range of the wall jet motions at  $x/H_j = 5$  are shown in Figure 9. The results show that the coherence between the pressure and vertical velocity component was larger as expected because the largest pressure source term in this region is normally  $dU/dydv/dx$ . The coherence  $\gamma_{pw}$  was large for positive and negative spacing but zero for  $\Delta z = 0$ . The fluctuating pressure and velocity components are not coherent for large separation distances  $\Delta z$  for any of the frequencies consistent with pressure results. This was true even for the frequency in the range of the wall jet motions. The results show that the nature of the lateral correlation for the frequency  $fX_r/U_j = 0.75$  was different from the motions with frequency of  $fX_r/U_j = 1.2$  particularly near the wall. The lateral coherence of the pressure and velocity is higher over an extended region in the case of the motions with  $fX_r/U_j = 0.75$ . There are also two distinct regions at different heights for these motions, where as the motions with  $fX_r/U_j = 1.2$  are centered at different heights. This results is consistent with the proposal of Gao and Ewing<sup>6</sup> that the motions may reflect different trajectories and phase velocities of the shear layer structures approaching the wall due to the flapping of the inner shear layer. The interplay between the contributions from these different modes maybe necessary to represent all the different trajectories of the motions.

The results for  $x/H_j = 8$  in the transition region for motions with frequency of  $fX_r/U_j = 0.28$ ,  $0.75$  and  $1.2$  are shown in figure 10. The results for the motions with  $fX_r/U_j = 0.75$  suggest that structures associated with the inner shear layer have grown both in vertical size and spanwise size as they evolve downstream. The regions with good coherence for  $fX_r/U_j = 0.75$  and  $1.2$  are again located at different positions further suggesting they may be complimentary. The dynamics of these motions<sup>15</sup> needs to be studied to better understand their roles. The fluctuating pressure and velocity for the frequency  $fH_j/U_j = 0.06$  ( $fX_r/U_j = 0.28$ ) associated with the wall jet motions were coherent over a much larger lateral distance than at  $x/H_j = 5$  suggesting that the motions at this frequency have grown much more two dimensional. The results at  $x/H_j = 12$  for  $fH_j/U_j = 0.06$ ,  $0.16$  and  $0.26$  are shown in figure 11. The results show that the lateral length scale of the wall jet structures have grown as they evolved downstream from  $x/H_j = 8$  to  $12$ . The coherence drops off rapidly for modest separation distances but is still significant for larger difference here suggesting there are both a three-dimensional component to the motion and a quasi two-dimensional mode, such as a braid-roller structures with quasi two-dimensional structures. This is consistent with investigation of the turbulent wall jet flow<sup>9,10</sup> that found evidence of highly two-dimensional structures. The coherence between the fluctuating pressure and velocity was largest for the vertical velocity over much of the flow. There was evident of a large coherence between the pressure and streamwise fluctuating velocity near the wall that was not evidence at  $x/H_j = 8$  that is likely due to the unsteady interaction of the structures with wall. This was consistent with the investigations of the planar wall jet that showed that the structures in the outer shear layer move toward the wall as the flow transitions to a fully developed wall jet flow<sup>10</sup> and the interaction of the structures with the wall resulted in unsteady separations near the wall.

## IV. Concluding Remarks

An experimental investigation was performed to characterize the three dimensionality of the flow structures in a planar offset jet initially issuing parallel to an adjacent wall with an offset distance of 1 jet height

and a Reynolds number of 44 000. The distributions of the mean velocity showed that the mean flow was two dimensional in an average sense in the central region of the jet ( $-4 \leq z/H_j \leq 4$ ) up to a streamwise location  $x/H_j = 12$ . The flow structures developed in the inner and the outer shear layer. The correlations of the fluctuating velocities and wall pressure showed that the flow structures in the shear layers of the attaching jet were three dimensional in the attachment region. The spanwise length scale of the flow structures was 1 to  $2H_j$  in the inner shear layer and 2 to  $3H_j$  in the outer shear layer. The flow structures in the inner shear layer gradually decreased in size and disappeared as the flow involved downstream. The flow structures in the outer shear layer grew in size and induced two dimensional motions near the wall. Eventually, the structures in the outer shear layer became similar to the fully developed wall jet structures.

## V. Acknowledgment

The first author acknowledges the support of the Natural Science Foundation of China (10802102).

## References

- <sup>1</sup>Lund T (1986) Augmented thrust and mass flow associated with two-dimensional jet reattachment. AIAA J 24:1964–1970.
- <sup>2</sup>Pelfrey J, Liburdy J (1986) Mean flow characteristics of a turbulent offset jet. J Fluids Eng 108:82–88.
- <sup>3</sup>Nasr A, Lai J (1997) Comparison of flow characteristics in the near field of two parallel plane jets and an offset plane jet. Phys Fluids 9:2919–2931.
- <sup>4</sup>Nasr A, Lai J (1998) A turbulent plane offset jet with small offset ratio. Exp in Fluids 24:47–57.
- <sup>5</sup>Gao N, Ewing D (2007) Experimental investigation of planar offset attaching jets with small offset distances. Exp. Fluids 42:941–954.
- <sup>6</sup>Gao N, Ewing D (2008) On the phase velocities of the motions in an offset attaching planar jet. J. Turbulence 9, 27:1–21.
- <sup>7</sup>Lee I, Ahn SK, Sung HJ(2004) Three-dimensional coherent structure in a separated and reattaching flow over a backward-facing step. Exp in Fluids 36:373–383
- <sup>8</sup>Kiya M, Sasaki K (1985) Structure of large-scale vortices and unsteady reverse flow in the reattaching zone of a turbulent separation bubble. J Fluid Mech 154:463–491.
- <sup>9</sup>Visbal MR, Gaitonde DV, Gogineni SP (1998) Direct numerical simulation of a forced transitional plane wall, AIAA paper 1998-2643
- <sup>10</sup>Gogineni SP, Visbal MR, Shih C (1999) Phase-resolved PIV measurements in a transitional plane wall jet: a numerical comparison, Exp in Fluids 27:126–136
- <sup>11</sup>Perry A (1982) Hot-wire Anemometry. Oxford: Clarendon Press.
- <sup>12</sup>Citriniti, J (1996) Experimental investigation into the large structures of the axisymmetric mixing layer using the proper orthogonal decomposition. PhD thesis, State University of New York at Buffalo, Amherst, NY.
- <sup>13</sup>Bruun, H. (1995) Hot-wire Anemometry. Oxford: Oxford University Press.
- <sup>14</sup>Bendat JS, Piersol AG (1993) Engineering applications of correlation and spectral analysis, NY:John Wiley and Sons,
- <sup>15</sup>Gao N, Ewing D (2010), Investigation of large scale flow structures in an offset attaching jet using spectral linear stochastic estimation, AIAA paper 2010-1290

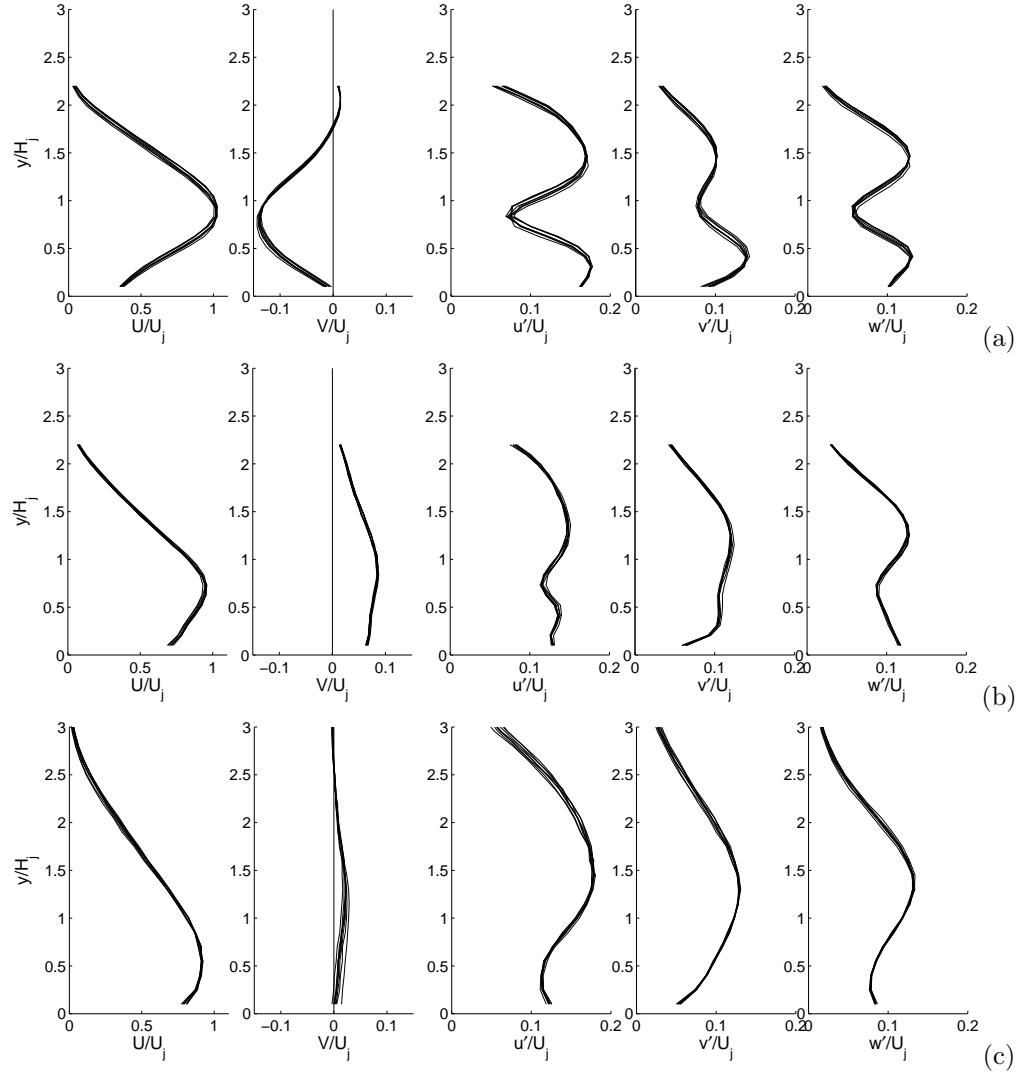


Figure 2. Comparison of the mean and the fluctuating velocities measured at  $-4 \leq z/H_j \leq 4$  for  $x/H_j =$  (a)5, (b)8 and (c)12 in the offset jet with  $H_s/H_j = 1.0$ .

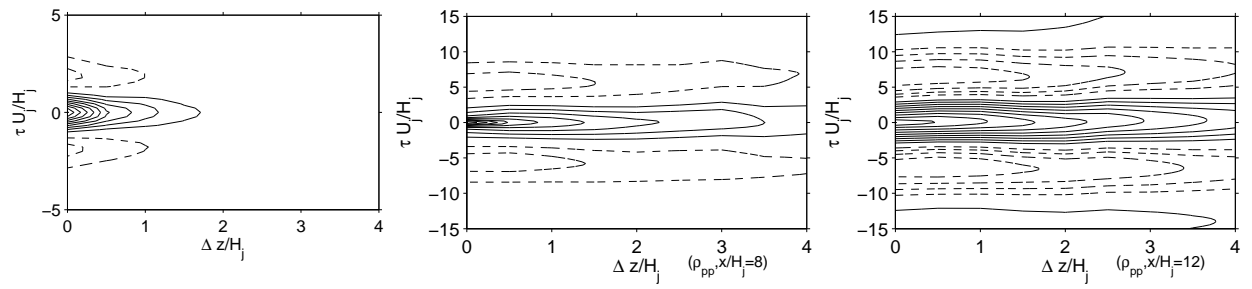
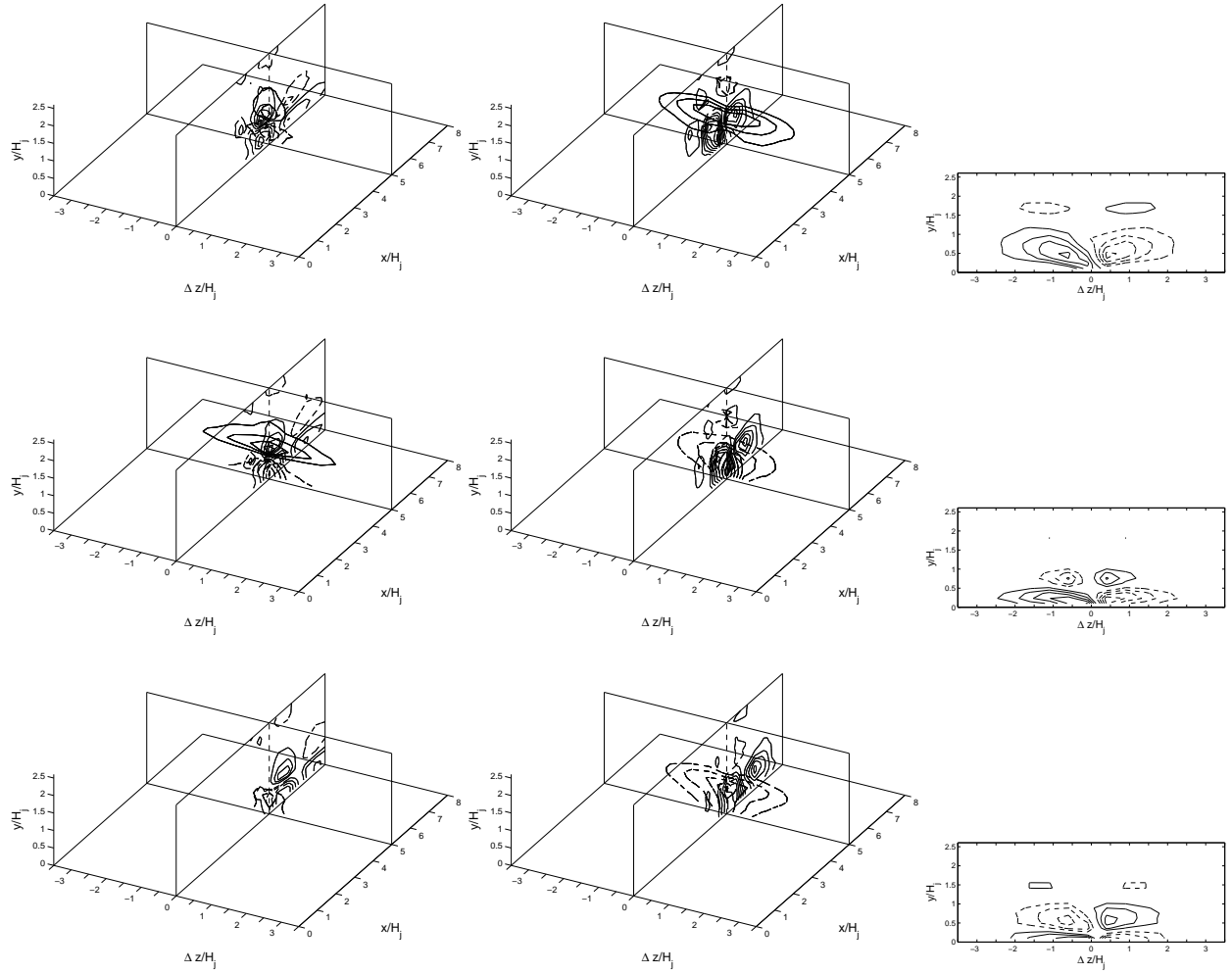
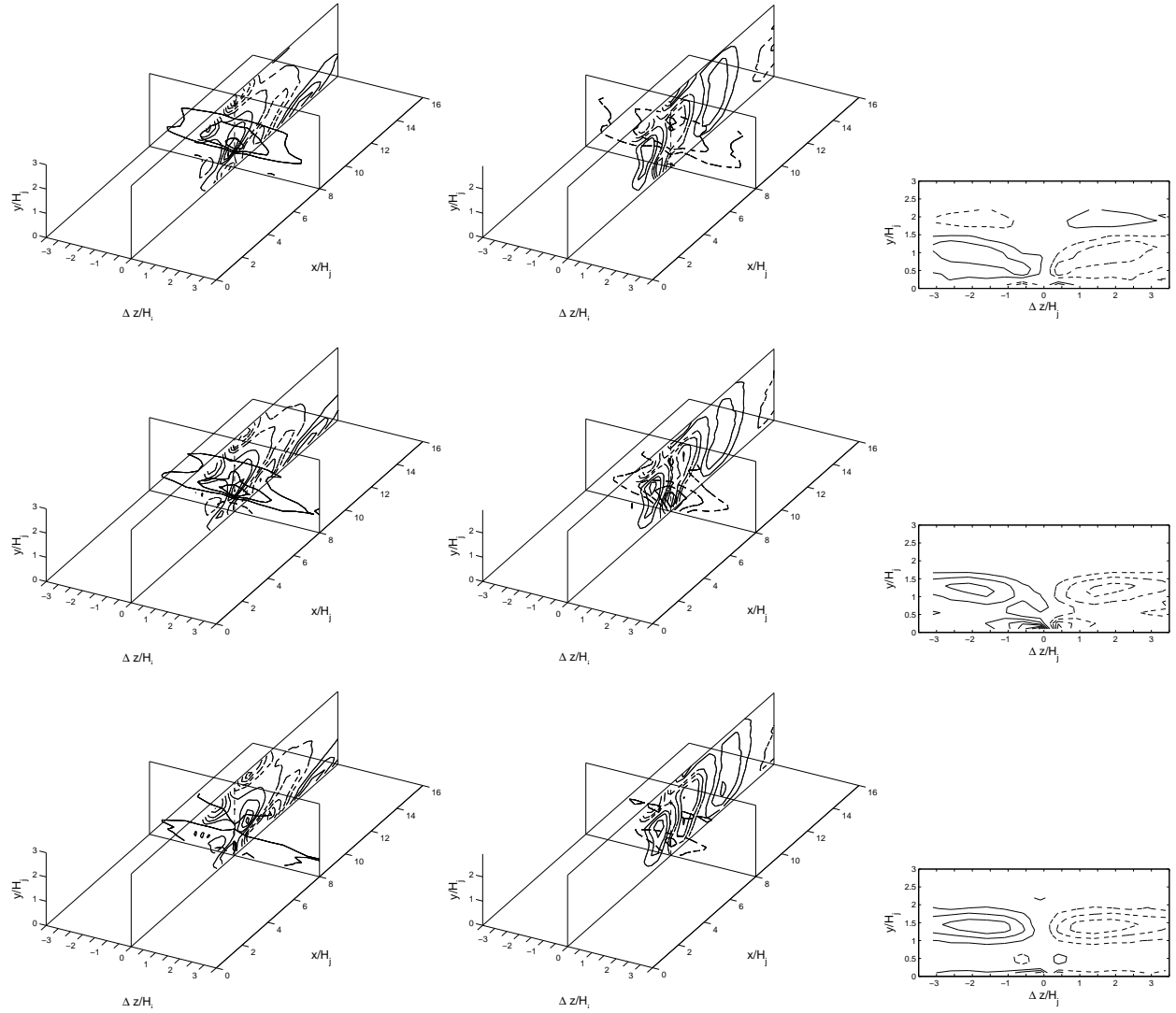


Figure 3. Correlation coefficients of the fluctuating wall pressure  $\rho_{pp}(x, \Delta z, \tau)$  for  $x/H_j = 5, 8$  and  $12$ . The cutoff contour is  $\pm 0.1$  and the contour interval is  $0.1$ .



**Figure 4.** Correlation coefficients of the fluctuating wall pressure and the fluctuating (left) streamwise velocity  $\rho_{pu}$ , (middle) vertical velocity  $\rho_{pv}$  and (right) lateral velocity  $\rho_{pw}$  for  $x/H_j = 5$  and three time intervals ( $\tau U_j/H_j = -0.9, 0$  and  $0.9$ , from top to bottom) in the offset jet with  $H_s/H_j = 1.0$ . Cutoff contour and contour interval are  $\pm 0.05$  and  $0.05$  for  $\rho_{pu}$  and  $\rho_{pv}$ , and  $\pm 0.025$  and  $0.025$  for  $\rho_{pw}$ .





**Figure 5.** Correlation coefficients of the fluctuating wall pressure and the fluctuating (left) streamwise velocity  $\rho_{pu}$ , (middle) vertical velocity  $\rho_{pv}$  and (right) lateral velocity  $\rho_{pw}$  for  $x/H_j = 8$  and three time intervals ( $\tau U_j/H_j = -0.9, 0$  and  $0.9$ , from top to bottom) in the offset jet with  $H_s/H_j = 1.0$ . Cutoff contour and contour interval are  $\pm 0.05$  and  $0.05$  for  $\rho_{pu}$  and  $\rho_{pv}$ , and  $\pm 0.025$  and  $0.025$  for  $\rho_{pw}$ .

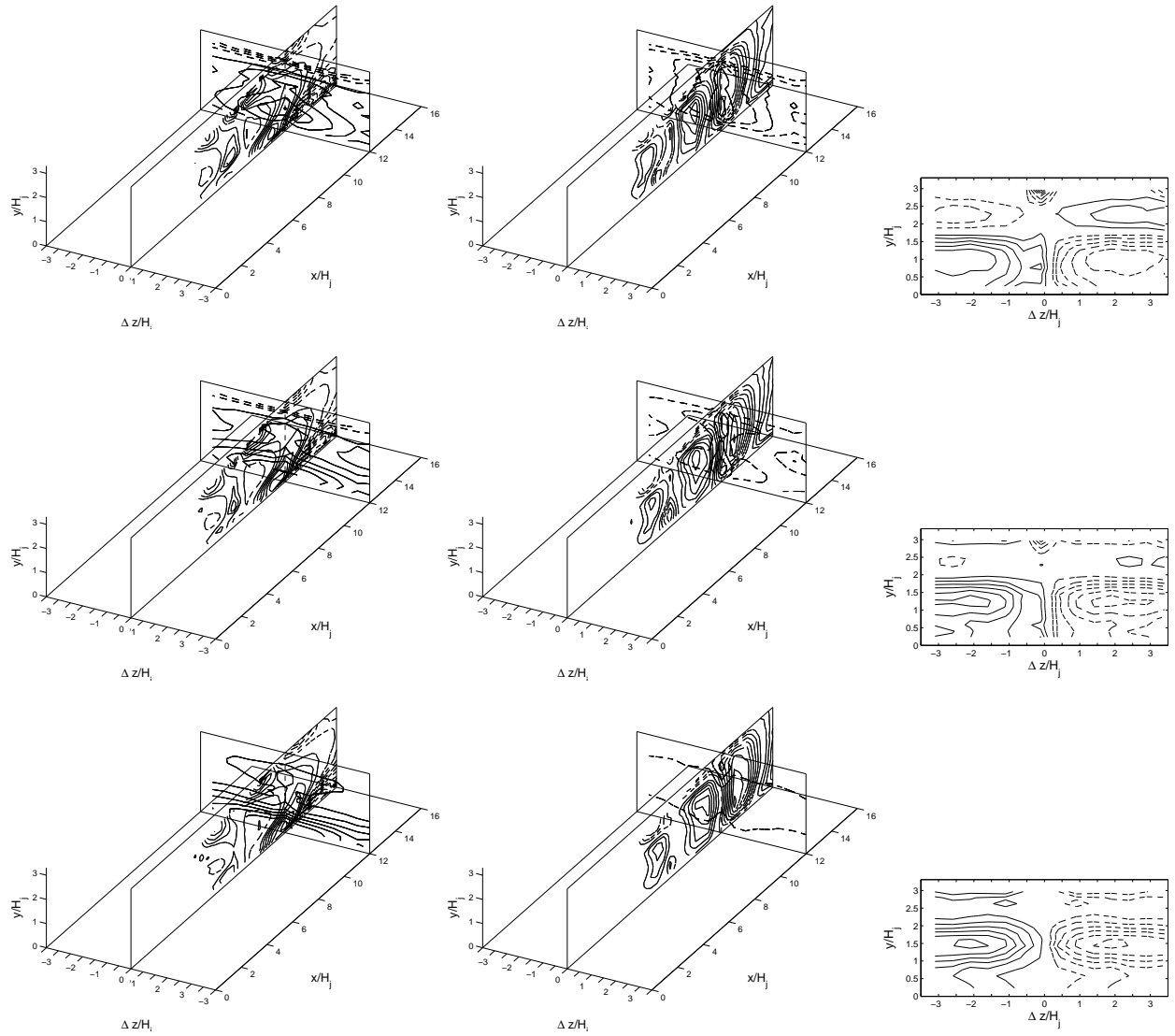


Figure 6. Correlation coefficients of the fluctuating wall pressure and the fluctuating (left) streamwise velocity  $\rho_{pu}$ , (middle) vertical velocity  $\rho_{pv}$  and (right) lateral velocity  $\rho_{pw}$  for  $x/H_j = 12$  and three time intervals ( $\tau U_j/H_j = -0.9, 0$  and  $0.9$ , from top to bottom) in the offset jet with  $H_s/H_j = 1.0$ . Cutoff contour and contour interval are  $\pm 0.05$  and  $0.05$  for  $\rho_{pu}$  and  $\rho_{pv}$ , and  $\pm 0.025$  and  $0.025$  for  $\rho_{pw}$ .

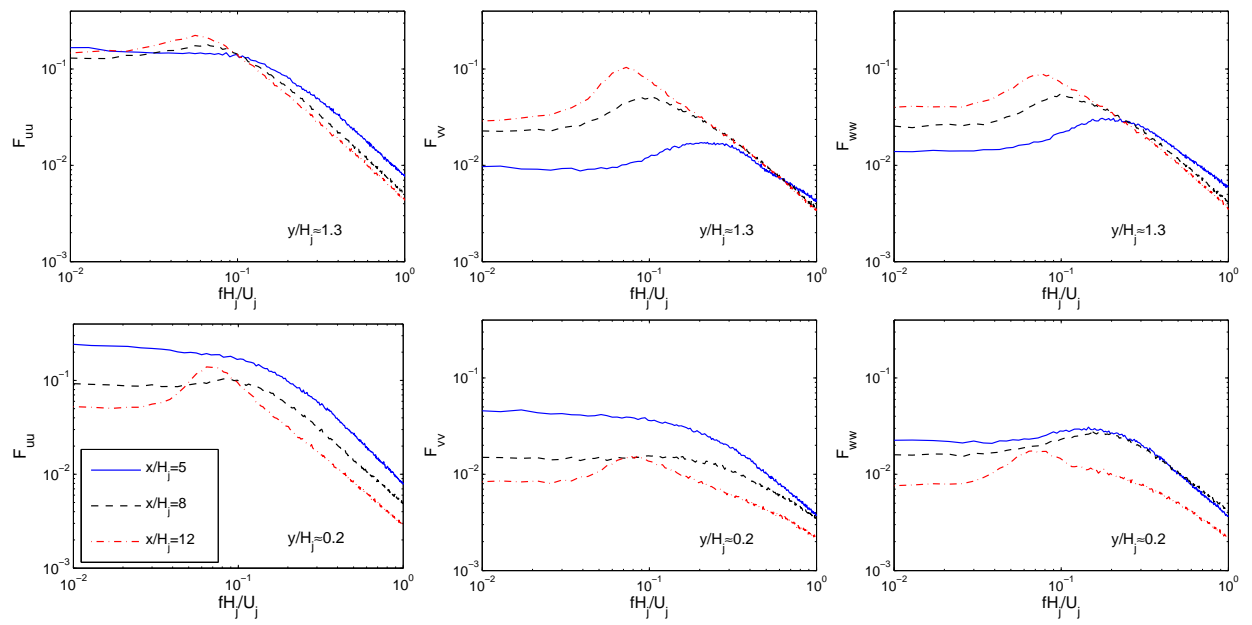


Figure 7. Spectra of the streamwise fluctuating velocities  $F_{uu}$ ,  $F_{vv}$  and  $F_{wv}$  for the offset jet with  $H_s/H_j = 1.0$  near the inner and the outer shear layer.

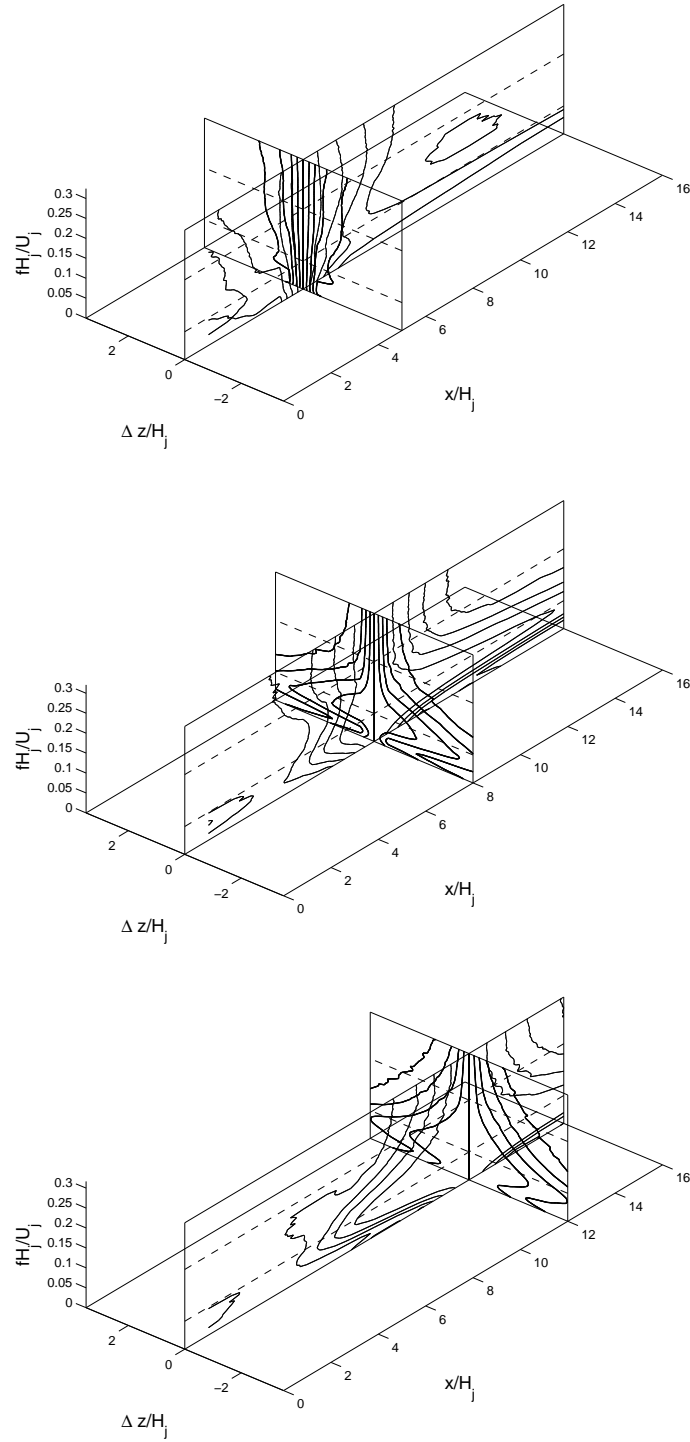


Figure 8. Coherence of the wall pressure  $\gamma_{pp}(x_1, x_2, \Delta z, f)$  for the reference location at  $x_1/H_j = 5, 8$  and  $12$  (top to bottom). The cutoff level is  $0.15$  and the contour interval is  $0.05$ . The dash lines indicate the frequencies of  $fH_j/U_j = 0.06$  and  $0.22$  ( $fX_r/U_j = 0.28$  and  $1.0$ ).

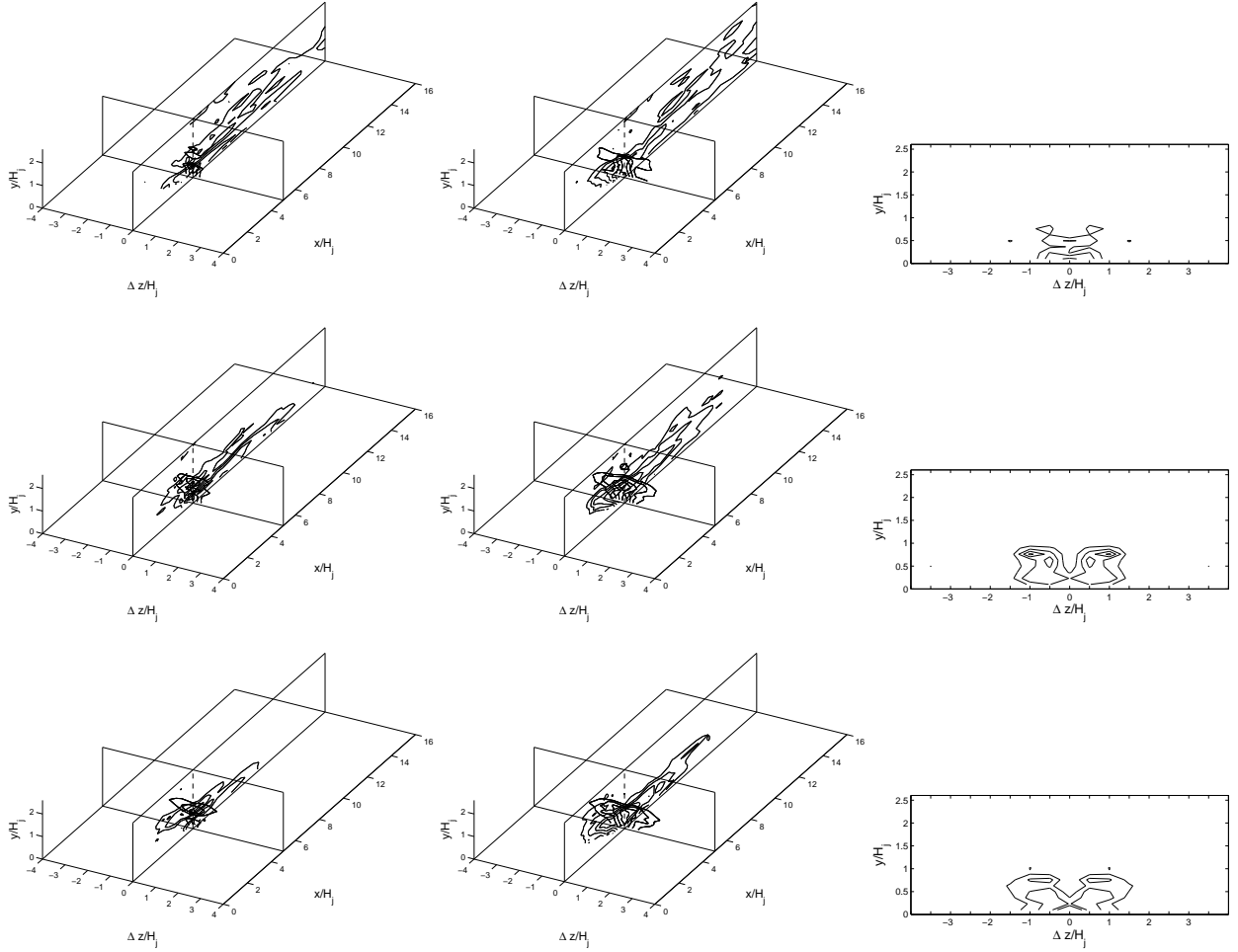
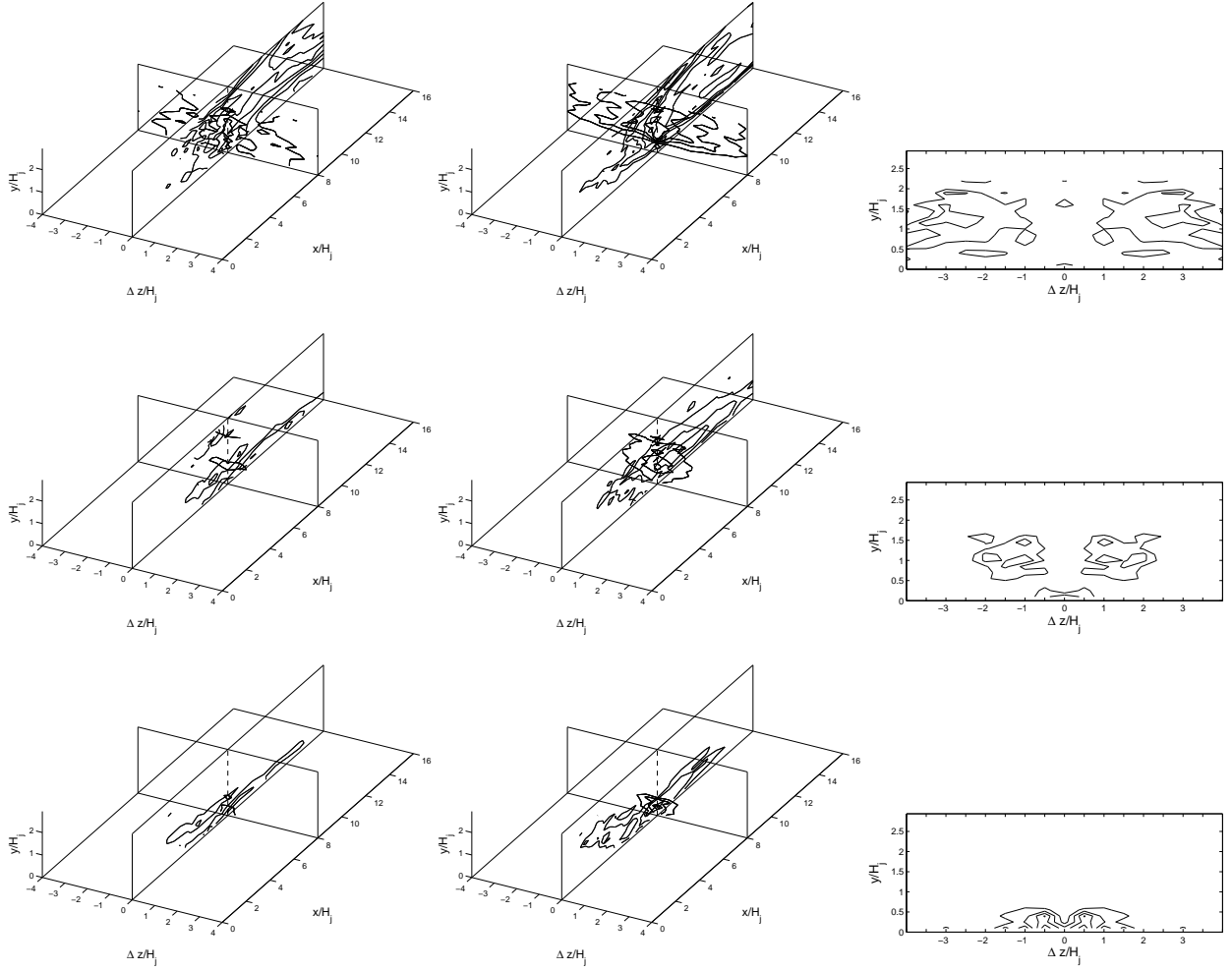


Figure 9. Coherence of the cross spectra between the fluctuating wall pressure and the fluctuating (left) streamwise velocity  $\gamma_{pu}$ , (middle) vertical velocity  $\gamma_{pv}$  and (right) lateral velocity  $\gamma_{pw}$  for  $x/H_j = 5$  and frequencies of  $fX_r/U_j = 0.28, 0.75$  and  $1.2$  ( $fH_j/U_j = 0.06, 0.16$  and  $0.26$ , from top to bottom) in the offset jet with  $H_s/H_j = 1.0$ . Cutoff contour and contour interval are  $\pm 0.2$  and  $0.1$  for  $\gamma_{pu}$  and  $\gamma_{pv}$ , and  $\pm 0.15$  and  $0.05$  for  $\gamma_{pw}$ .



**Figure 10.** Coherence of the cross spectra between the fluctuating wall pressure and the fluctuating (left) streamwise velocity  $\gamma_{pu}$ , (middle) vertical velocity  $\gamma_{pv}$  and (right) lateral velocity  $\gamma_{pw}$  for  $x/H_j = 8$  and frequencies of  $fX_r/U_j = 0.28, 0.75$  and  $1.2$  ( $fH_j/U_j = 0.06, 0.16$  and  $0.26$ , from top to bottom) in the offset jet with  $H_s/H_j = 1.0$ . Cutoff contour and contour interval are  $\pm 0.2$  and  $0.1$  for  $\gamma_{pu}$  and  $\gamma_{pv}$ , and  $\pm 0.15$  and  $0.05$  for  $\gamma_{pw}$ .

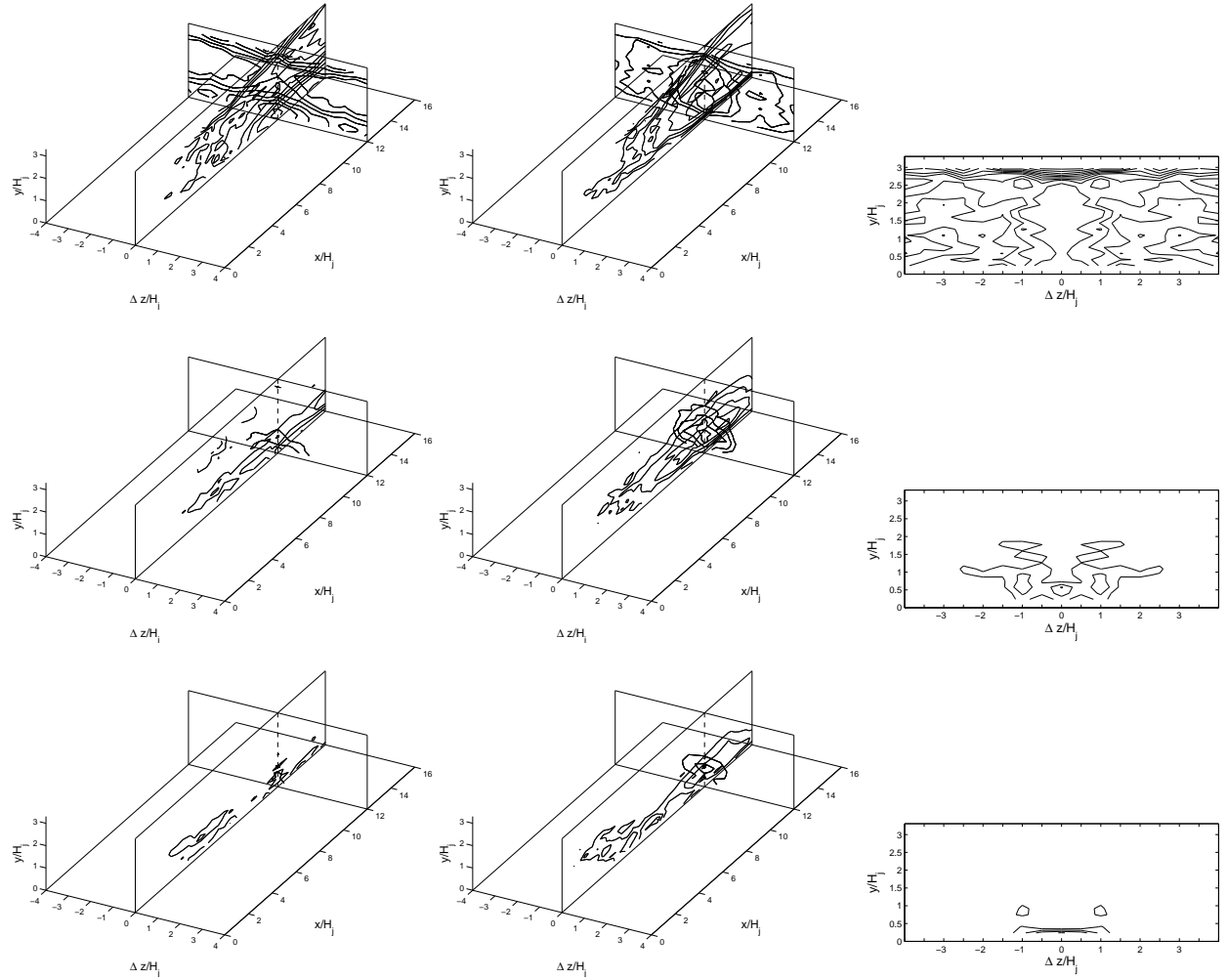


Figure 11. Coherence of the cross spectra between the fluctuating wall pressure and the fluctuating (left) streamwise velocity  $\gamma_{pu}$ , (middle) vertical velocity  $\gamma_{pv}$  and (right) lateral velocity  $\gamma_{pw}$  for  $x/H_j = 12$  and frequencies of  $fX_r/U_j = 0.28, 0.75$  and  $1.2$  ( $fH_j/U_j = 0.06, 0.16$  and  $0.26$ , from top to bottom) in the offset jet with  $H_s/H_j = 1.0$ . Cutoff contour and contour interval are  $\pm 0.2$  and  $0.1$  for  $\gamma_{pu}$  and  $\gamma_{pv}$ , and  $\pm 0.15$  and  $0.05$  for  $\gamma_{pw}$ .